NOTE: This is a draft of a paper being submitted for publication. Contents of this paper should not be quoted nor referred to without permission of the authors.

Conf-830120--1

CONF-830120--1

DE83 006138

SURFACE PROBE MEASUREMENTS IN ISX-B AND EBT-S

R. A. Zuhr

SOLID STATE DIVISION
OAK RIDGE NATIONAL LABORATORY
Operated by
UNION CARBIDE CORPORATION
Under
Contract No. W-7405-eng-26
With the
U. S. DEPARTMENT OF ENERGY
OAK RIDGE, TENNESSEE

December 1982

SURFACE PROBE MEASUREMENTS IN ISX-B AND EBT-S*

R. A. Zuhr
Solid State Division
Oak Ridge National Laboratory
Oak Ridge, Tennessee 37830

1. Introduction

The processes that take place in the scrapeoff layer of a magnetic confinement fusion experiment strongly influence the overall performance of the machine. Improved understanding of these processes can be achieved by plasma edge measurements using deposition probes that are analyzed by surface physics techniques. At ORNL a series of *in situ* surface deposition probe measurements has been made on the ISX-B tokamak and the Elmo bumpy torus, EBT-S. The goal of these measurements is to gain insight into the mechanisms of impurity introduction and hydrogen recycle by characterizing impurity and plasma fluxes in the edge, by measuring edge erosion rates, and by determining the effects of machine operating parameters on the edge plasma. This paper is a summary of recent surface probe results obtained in ISX-B and EBT-S using accelerator based analysis techniques.

2. Experimental Procedure

Both stationary and time-resolved (15 ms) surface probes are exposed in the scrapeoff layers of ISX-B and EBT-S. The deposition samples are single crystal silicon for impurity collection and amorphous silicon for deuterium trapping. After exposure the samples are analyzed using accelerator based techniques (1-3). Retained amounts are determined using Rutherford ion backscattering (RBS) with 2 MeV ^{4}He in a channeling configuration for impurities and nuclear reaction analysis (NRA) with the D(^{3}He,p)^{4}He reaction for deuterium. Deuterium energies are evaluated from depth profiling (1), trapping vs. fluence curves (1, 4), single crystal damage (5) and transmission through limiting apertures (6). Quantitative results are readily obtained with sensitivities of $\sim 10^{13}$ atoms/cm^2 for heavy impurities and 10^{15}/cm^2 for light impurities and deuterium.

3. Results and Discussion - ISX-B

A summary of the results of surface probe measurements in the scrapeoff layer of ISX-B is presented in Table 1. These data are for non-gettered ohmic discharges with density $\bar{n}_e \approx 4 \times 10^{13}/\text{cm}^3$, magnetic field $B_T \approx 1.3$ T, and plasma current $I_p \approx 150$ kA.

The circulating plasma ion flux and energy at 2 cm behind the limiter ($\sim 2 \times 10^{18}/\text{cm}^2$-s at 20 eV Maxwellian) were determined by fitting

---

*Research sponsored by Union Carbide Corporation under contract W-7405-eng-26 with the U. S. Department of Energy.

the experimental data to a revised trapping vs. fluence model (7, 8). The saturation behavior in such a model indicates that the incident distribution is Maxwellian and not monoenergetic. The measured edge ion temperature of 20 eV is comparable to edge electron temperatures (10-40 eV) measured using Langmuir probes (9) and Thomson scattering (10). The measured ion flux is in agreement with the ion saturation current ($3 \times 10^{18}/cm^2$-s) to a biased probe at the same radius (10). The scrapeoff length of the ion flux as measured with surface probes (2 cm) is also in agreement with the 1.9 cm 1/e decay length of the ion saturation current (10).

Table I

Typical ISX-B edge parameters inferred from surface probe measurements for non-gettered, ohmic plasmas with $\bar{n} \approx 4 \times 10^{13}/cm^3$, $I_p \approx 150$ kA, and $B_T \approx 1.3$ T.

<u>2 cm outside limiter radius</u>		
Ion density	$2 \times 10^{12}/cm^3$	ref. 4
Ion temperature	20 eV, Maxwellian	ref. 4
Circulating ion flux	$2 \times 10^{18}/cm^2$-s	ref. 4
Circulating impurity fluxes:		
Oxygen	2-5 $\times 10^{16}/cm^2$-s	ref. 1,2
Iron	2-5 $\times 10^{15}/cm^2$-s	ref. 1,2
Carbon	$2 \times 10^{15}/cm^2$-s	ref. 1
Titanium (with TiC limiter)	$4 \times 10^{14}/cm^2$-s	ref. 2
Flux scrapeoff length:		
Hydrogen and Iron	2 cm	ref. 1
Surface erosion rate (Au)	$2 \times 10^{15}/cm^2$-s	ref. 3
<u>At outer wall position (away from limiter)</u>		
Neutral hydrogen flux to wall	$2 \times 10^{16}/cm^2$-s	ref. 4
Neutral energy	30 eV (with high E tail)	ref. 4
Iron impurity deposition	$<10^{12}/cm^2$-s	ref. 4
Surface erosion rate (Au)	$<10^{14}/cm^2$-s	ref. 3

Deposition probe measurements at and behind the vacuum vessel wall indicate that the charge exchange neutral flux reaching the wall is $2 \times 10^{16}/cm^2$-s at ~30 eV. This flux is consistent with estimates of the particle balance in ISX-B if a confinement time of ~20 ms is assumed. The enhanced high energy tail of the distribution is consistent with conventional high energy charge exchange measurements (11). A recent attempt to extend charge exchange measurements to lower energies gives a flux of ~$5 \times 10^{15}/cm^2$-s at energies above 35 eV (12). This result is also consistent with the present data since the flux is continuing to rise with decreasing energy.

For non-gettered discharges the principal impurities found in the plasma edge are oxygen, carbon, and the components of stainless steel, with a lesser amount of titanium from the TiC coated mushroom limiter. The measured oxygen flux represents 1% of the plasma density, while iron and carbon are a factor of 10 lower. The edge iron density is an order of magnitude higher than the iron density in the center of the plasma as measured by optical spectroscopy (13). This indicates that the scrapeoff layer is effective in screening metallic impurities from the plasma core.

Heavy impurities are a factor of 3 higher in deuterium plasmas than in hydrogen plasmas, while oxygen levels remain the same (14). This suggests that sputtering is the principal source of metallic impurities while chemical effects are important in the case of oxygen. The low measured density of limiter material (Ti) in the edge relative to the wall material (Fe) demonstrates that the wall and not the limiter is the main source of metallic impurities. These results suggest an impurity introduction model in which charge exchange neutral sputtering of the wall is the dominant mechanism (4). If a sputtering coefficient of 10^{-3} is assumed (15) such a model can account for the circulating iron flux in the edge. The sputtered iron flux will then be $\sim 2 \times 10^{13}$/cm^2-s, an order of magnitude higher than the maximum rate of iron redeposition on the wall (4). Thus the wall away from the limiter is a source and not a sink for metallic impurities. This conclusion is also in agreement with plasma shifting experiments (16).

Several time-resolved experiments have been done on ISX-B to investigate the effects of neutral beam injection (NBI) and gas puffing on plasma and impurity fluxes in the edge (2). In Fig. 1 impurity deposition rates for 1.1 MW beam injected discharges are plotted vs time.

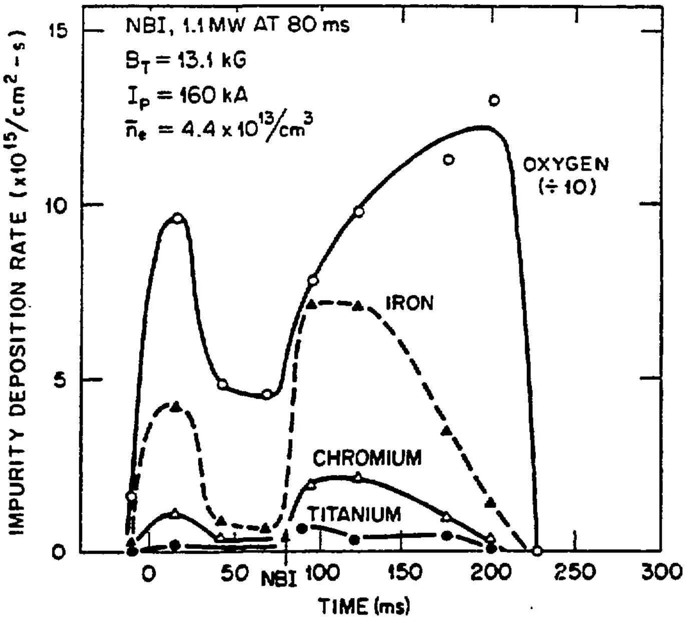

Fig. 1. Time-resolved impurity deposition rate for 1.1 MW NBI discharges in ISX-B. The arrow indicates the start of the 100 ms NBI.

With the onset of NBI at 80 ms there is an order of magnitude increase in metallic impurity fluxes. Toward the end of the discharge the iron and oxygen fluxes diverge, providing a further indication that different processes are important in the introduction of these two elements. Time-resolved measurements made to determine the effects of gas puffing on the edge plasma show a factor of two decrease in plasma flux immediately after a sharp 0.3 tl puff. This indicates that the scrapeoff layer is cooled by gas puffing. Impurity fluxes during the same discharges show only minor decreases at the time of the puff. Thus gas puffing cools the plasma edge and maintains plasma stability but does not substantially affect edge impurity levels.

4. Results and Discussion EBT-S

In any magnetically confined plasma the ions travel between collisions in spiral paths along the magnetic field lines. The radius of this spiral orbit is a function of the ion energy. In EBT-S an aperture transmission experiment which selectively measures this gyroradius was used to determine the deuterium energy and flux 15 mm from the wall in the midplane of a sector (6). Measurements were made in both toroidal directions and the results are shown in Fig. 2. The measured transmission of deuterium through a circular aperture (circles and squares) is plotted as a function of the distance from the axis. The solid curve is the calculated transmission for a 20 eV Maxwellian incident energy distribution with a 3 kT sheath potential. The fit is good except at the edge of the distribution closest to the plasma where the data lie slightly above the calculation, indicating an enhancement in the number of high energy particles. The incident flux was determined from saturation effects to be $\sim 10^{17}/\text{cm}^2\text{-s}$. Laser fluorescence measurements of neutral aluminum in the same region show that aluminum, the principal impurity in EBT, enters the plasma via sputtering (17). The two sets of data together indicate that the deuterium flux alone is not sufficient to do the sputtering and that aluminum self-sputtering is the most likely impurity introduction mechanism in EBT-S.

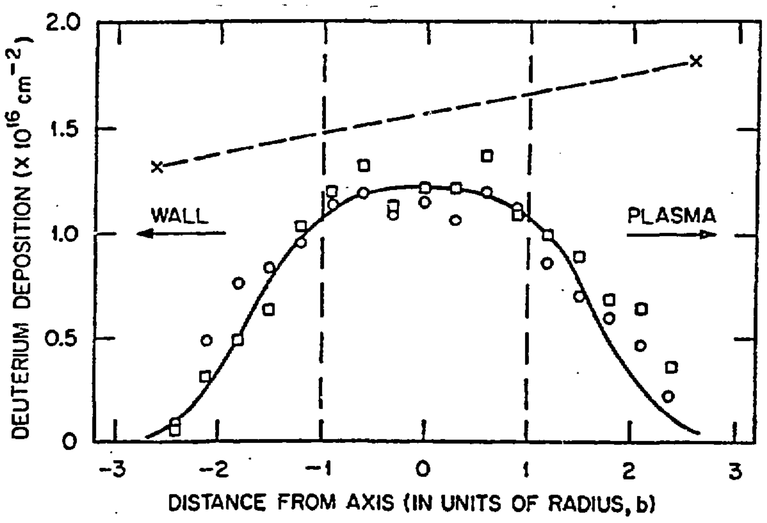

Fig. 2. Deuterium transmission through an aperture of radius b facing cw (O) and ccw (□) in EBT-S. The solid curve is the calculated transmission for kT = 20 eV with a 3 kT sheath potential.

5. Conclusion

Surface deposition probe techniques have been shown to be an effective means of determining the characteristics of the plasma edge region of magnetic confinement devices. Experimental results on ISX-B and EBT-S have led to a consistent picture of the edge plasma and the dominant impurity introduction mechanisms. This picture is supported by numerous other measurements and emphasizes the importance of concentrating several techniques on the complex problems of plasma fusion.

REFERENCES

1. R. A. Zuhr, S. P. Withrow, and J. B. Roberto, J. Nucl. Mater. 93-94, 127 (1980).
2. R. A. Zuhr, J. B. Roberto, and S. P. Withrow, J. Nucl. Mater. 103-104, 315 (1981).
3. J. B. Roberto, R. A. Zuhr, and S. P. Withrow, J. Nucl. Mater. 93-94, 146 (1980).
4. R. A. Zuhr, J. B. Roberto, and S. P. Withrow, J. Vac. Sci. Technol. 20, 1244 (1982).
5. S. P. Withrow, R. A. Zuhr, and J. Roth, J. Vac. Sci. Technol. 20, 1323 (1982).
6. R. A. Zuhr, R. E. Clausing, L. Heatherly, and R. K. Richards, J. Nucl. Mater. 111-112, 177 (1982).
7. S. A. Cohen and G. M. McCracken, J. Nucl. Mater. 84, 157 (1979).
8. W. R. Wampler, Sandia National Laboratories, private communication.
9. W. Namkung, A. C. England, and O. C. Eldridge, ORNL-TM6621, Oak Ridge, TN (1978).
10. P. K. Mioduszewski, P. H. Edmonds, and J. Sheffield, J. Vac. Sci. Technol. 20, 1284 (1982).
11. S. D. Scott, Oak Ridge National Laboratory, private communication.
12. D. E. Thomas, Oak Ridge National Laboratory, private communication.
13. R. C. Isler, Oak Ridge National Laboratory, private communication.
14. J. B. Roberto, R. C. Isler, S. Kasai, L. E. Murray, J. E. Simpkins, S. P. Withrow, and R. A. Zuhr, J. Nucl. Mater. 103-104, 531 (1981).
15. J. Roth, J. Bohdansky, and W. Ottenberger, Max Planck Institut fur Plasmaphysik Report IPP 9/26 (1979).
16. R. C. Isler, S. Kasai, L. E. Murray, M. J. Saltmarsh, and M. Murakami, Phys. Rev. Lett. 47, 333 (1981).
17. E. Dullni, E. Hintz, J. B. Roberto, R. J. Colchin, and R. K. Richards, J. Nucl. Mater. 111-112, 61 (1982).